Japanese Journal of Applied Physics 56, 078002 (2017)
https://doi.org/10.7567/JJAP.56.078002

BRIEF NOTE

Temperature sensing based on multimodal interference in polymer optical fibers: Room-temperature sensitivity enhancement by annealing

Tomohito Kawa[1], Goki Numata[1], Heeyoung Lee[1], Neisei Hayashi[2], Yosuke Mizuno[1*], and Kentaro Nakamura[1]

[1]Institute of Innovative Research, Tokyo Institute of Technology, Yokohama 226-8503, Japan
[2]Research Center for Advanced Science and Technology, The University of Tokyo, Meguro, Tokyo 153-8904, Japan

*E-mail: ymizuno@sonic.pi.titech.ac.jp

Received February 15, 2017; accepted May 19, 2017; published online June 13, 2017

To date, we have developed a temperature sensor based on multimodal interference in a polymer optical fiber (POF) with an extremely high sensitivity. Here, we experimentally evaluate the influence of annealing (heat treatment) of the POF on the temperature sensitivity at room temperature. We show that the temperature sensitivity is enhanced with increasing annealing temperature, and that, by annealing the POF at 90 °C, we can achieve a temperature sensitivity of +2.17 nm/°C, which is 2.9 times larger than that without annealing (+0.75 nm/°C).

Researchers have developed various types of fiber-optic interference-based temperature sensors,[1–3] among which those based on multimodal interference in multimode fibers (MMFs) have gained considerable attention for two decades on account of their advantages, such as system simplicity, cost efficiency, and high sensitivity.[4–22] A lot of configurations have been reported so far (summarized in Ref. 7), and one of the types that can be most easily implemented is categorized as "single-mode-multimode-single-mode" (SMS) type,[7–24] in which an MMF is simply sandwiched between two single-mode fibers (SMFs).

Let us review the recent developments of SMS-based temperature sensors. Ten years ago, using a 1.8-m-long silica graded-index (GI-) MMF, a temperature sensitivity of +58.5 pm/°C was obtained at 1550 nm.[8] Two years later, the relationship between the temperature sensitivity and the optical wavelength was partially clarified, and both the absolute value and the sign of the sensitivity were found to depend on so-called "critical wavelengths",[9] which are influenced by the core diameter and/or the dopant of silica MMFs. In 2012, a polymer optical fiber (POF) was first employed as the MMF to be sandwiched between two SMFs; when a 0.16-m-long poly(methyl methacrylate) (PMMA)-based step-index POF was used, a temperature sensitivity of −56.8 pm/°C was obtained at 1570 nm.[21] However, the extremely high propagation loss of PMMA-based POFs at ∼1300 and ∼1550 nm (≫100 dB/m)[25] limited the transmitted optical power, resulting in a lower signal-to-noise ratio of the measurement.

To overcome this problem, since 2014, we have been studying SMS-based temperature sensing using perfluorinated (PF) GI-POFs,[22–24] which are the only POFs with a relatively low loss even at 1300 nm (∼0.05 dB/km) and at 1550 nm (∼0.25 dB/m).[26] Using a PFGI-POF with a length of 1.0 m and a core diameter of 120 μm, we obtained a temperature sensitivity of +0.74 nm/°C at room temperature at 1300 nm,[22] the absolute value of which is more than 15 times the value reported using silica MMFs.

We also found that the absolute value of the temperature sensitivity is significantly enhanced with increasing temperature toward ∼80 °C,[23] which is close to the glass-transition temperature (∼100 °C) of the core polymer.[27] For instance, when the core diameter was 120 μm, the sensitivity at 82 °C at 1300 nm was 85.6 nm/°C, which is ∼78 times the value obtained at room temperature and more than 1500 times the value previously reported using a silica MMF. This dramatic rise in the temperature sensitivity appears to be caused by the fact that the physical properties (core diameter, fiber length, refractive index, etc.) of the POF are altered at the temperature several tens of degrees lower than the glass-transition temperature.[28] This physical change is probably irreversible and may have some influence on the temperature sensitivity at room temperature, but no report has been provided thus far. Note that the sensitivity of POF-based pressure sensors has been reported to be improved by annealing of the POF in advance.[29]

In this work, we experimentally evaluate the influence of annealing (heat treatment) of the POF on the temperature sensitivity at room temperature. The temperature sensitivity is found to be enhanced with increasing annealing temperature. We obtain a temperature sensitivity of +2.17 nm/°C by annealing the POF at 90 °C, which is 2.9 times the value without annealing (+0.75 nm/°C).

In an SMS structure, the light incident from an SMF to an MMF excites a few lower modes in the MMF, because the spot-sizes are different between the fundamental or the 0th modes in the SMF and the MMF. The excited modes propagate along the MMF, tracing their respective paths, and reach the other MMF-to-SMF boundary. Here, the net field coupled to the SMF depends on the relative phase differences among the multiple modes that have propagated along the MMF. If we assume that the MMF and the two SMFs are all axially aligned, the modes excited in the MMF can be considered to be axially symmetric, and the optical power P_{out} output from the SMS structure is given as[10]

$$P_{\mathrm{out}} = |a_0^2 + a_1^2 \exp i(\beta_0 - \beta_1)L + a_2^2 \exp i(\beta_0 - \beta_2)L + \cdots|^2, \tag{1}$$

where i denotes an integer, a_i the field amplitudes of the i-th modes at the first SMF-to-MMF boundary, β_i the propagation constants of the i-th modes, and L the MMF length. According to Eq. (1), it is clear that the optical output power depends on the physical changes caused by temperature; and consequently, temperature sensing turns out feasible by measuring the shift of spectral dips or peaks.

In the experiment, as an MMF in the SMS structure, we employed 0.3-m-long PFGI-POFs with a core diameter of 120 μm. The experimental setup is schematically shown in Fig. 1. A swept-source laser (SSL; sweep rate: 20 kHz; central wavelength: 1320 nm; bandwidth: 110 nm) was used as a broadband light source. Before injection to the POF, the

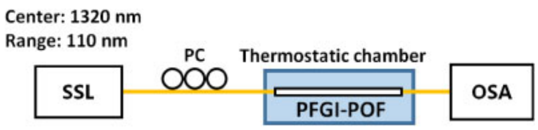

Fig. 1. (Color online) Schematic of experimental setup. OSA, optical spectrum analyzer; PC, polarization controller; PFGI-POF, perfluorinated graded-index polymer optical fiber; SSL, swept-source laser.

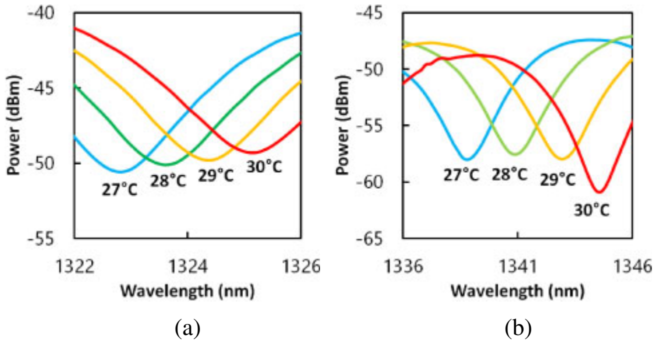

Fig. 2. (Color online) Temperature dependences of the spectral dip measured at room temperature (a) before and (b) after 90 °C annealing.

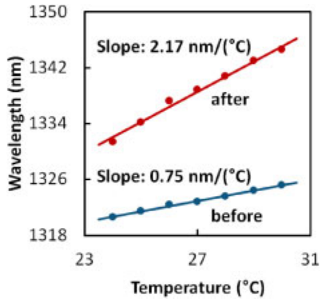

Fig. 3. (Color online) Dip wavelength measured with respect to temperature before and after 90 °C annealing. The solid lines are linear fits.

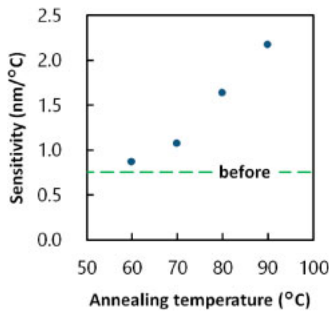

Fig. 4. (Color online) Temperature sensitivity at room temperature plotted as a function of annealing temperature.

laser output was input to a polarization controller (PC) so that the polarization-dependent spectral fluctuations[8] were suppressed. The laser output was then injected to the POF via an "SC/PC-FC/PC" adaptor, at which the ends of the POF and the SMF were butt-coupled to each other.[30] The other POF-to-SMF boundary was also butt-coupled in the same manner. The spectrum of the transmitted light was finally monitored using an optical spectrum analyzer (OSA). The entire length of the POF was placed in a thermostatic chamber; each POF sample was annealed at 60, 70, 80, 90, 100 °C for 1 h [excluding the temperature rising and falling durations (approximately 30 and 10 min, respectively); sufficiently long for measured data saturation], and then the temperature sensitivity around room temperature (27 °C) was measured.

Figures 2(a) and 2(b) show the temperature dependences of the spectral dip at room temperature before and after annealing at 90 °C, respectively. The clearest dips that appeared around the central wavelength of the light source were selected. In both the figures, the dips shifted to longer wavelength with increasing temperature. The temperature dependences of the central wavelengths of the dips are shown in Fig. 3. The dependences were both almost linear before and after annealing, however the temperature sensitivity before annealing was +0.75 nm/°C (which agrees well with the previously obtained value),[22] while that after annealing was +2.17 nm/°C; 2.9 times sensitivity enhancement was obtained by annealing at 90 °C.

We also attempted to perform the same measurement when the annealing temperature was 60, 70, 80, and 100 °C. The measurement was successful in the cases of 60, 70, and 80 °C; but the POF was melted during annealing at 100 °C, inducing such a high loss that no light was able to propagate through the POF. The annealing temperature dependence of the temperature sensitivity at room temperature is shown in Fig. 4. With increasing annealing temperature, the temperature sensitivity at room temperature was enhanced, probably because the change in the physical properties of the polymer becomes striking as the annealing temperature is close to the glass-transition temperature. If users pursue a higher sensitivity, an annealing temperature of 90 °C is the most suitable of all the five temperatures tested in our experiment, because the measurement was still performed with a moderate signal-to-noise ratio only with ∼10-dB loss [Fig. 2(b)]. Even at 60 °C annealing, we observed slight increase in the sensitivity, which is within the inevitable measurement error caused by the SMF-to-POF coupling conditions different sample by sample.[22–24] Though we have to admit that this measurement is only for PFGI-POFs with particular physical and structural properties, we can still draw a more general conclusion that the temperature sensing performance of POF-based SMS sensors is to some extent controllable by annealing. It should be also noted that our measurement result does not necessarily indicate that the measurable temperature range of SMS-based sensors using POFs is limited up to ∼60 °C, because once POFs are annealed, their sensing properties may not be affected in the temperature range below the annealing temperature. In this meaning, annealing could be regarded as a method of increasing the upper limit of the measurable temperature range.

In summary, regarding the SMS-based temperature sensors using POFs, we evaluated the influence of annealing of the POF on the temperature sensitivity at room temperature. When a 0.3-m-long PFGI-POF with a core diameter of 120 μm was used, the temperature sensitivity was enhanced with increasing annealing temperature. A temperature sensitivity of +2.17 nm/°C was achieved by annealing the POF at 90 °C. This value was 2.9 times larger than that without annealing (+0.75 nm/°C). Thus, we believe that annealing is a useful technique for improving (or controlling) the temperature sensitivity at room temperature of POF-based SMS sensors.

Acknowledgments This work was supported by JSPS KAKENHI Grant Numbers 25709032, 26630180, 25007652, 17J07226, and 17H04930, and by research grants from the Japan Gas Association, the ESPEC Foundation for Global Environment Research and Technology, and the Association for Disaster Prevention Research.

1) Y. J. Rao, D. A. Jackson, L. Zhang, and I. Bennion, Opt. Lett. **21**, 1556 (1996).
2) Y. Chen and H. F. Taylor, Opt. Lett. **27**, 903 (2002).
3) Y. Mizuno, N. Hayashi, H. Fukuda, K. Y. Song, and K. Nakamura, Light: Sci. Appl. **5**, e16184 (2016).
4) E. Li, X. Wang, and C. Zhang, Appl. Phys. Lett. **89**, 091119 (2006).
5) A. Mehta, W. Mohammed, and E. G. Johnson, IEEE Photonics Technol. Lett. **15**, 1129 (2003).
6) R. M. Ribeiro and M. M. Werneck, Sens. Actuators A **111**, 210 (2004).
7) O. Frazão, S. O. Silva, J. Viegas, L. A. Ferreira, F. M. Araújo, and J. L. Santos, Appl. Opt. **50**, E184 (2011).
8) Y. Liu and L. Wei, Appl. Opt. **46**, 2516 (2007).
9) S. M. Tripathi, A. Kumar, R. K. Varshney, Y. B. P. Kumar, E. Marin, and J. P. Meunier, J. Lightwave Technol. **27**, 2348 (2009).
10) A. Kumar, R. K. Varshney, S. Antony C, and P. Sharma, Opt. Commun. **219**, 215 (2003).
11) M. Kumar, A. Kumar, and S. M. Tripathi, Opt. Commun. **312**, 222 (2014).
12) S. M. Tripathi, A. Kumar, E. Marin, and J. P. Meunier, IEEE Photonics Technol. Lett. **22**, 799 (2010).
13) Q. Wu, Y. Semenova, P. Wang, and G. Farrell, Opt. Express **19**, 7937 (2011).
14) Y. Chen, Q. Han, T. Liu, X. Lan, and H. Xiao, Opt. Lett. **38**, 3999 (2013).
15) Y. Gong, T. Zhao, Y. J. Rao, and Y. Wu, IEEE Photonics Technol. Lett. **23**, 679 (2011).
16) E. Li, Opt. Lett. **32**, 2064 (2007).
17) A. K. Chotimah, A. M. Hatta, and D. Y. Pratama, Proc. SPIE **10150**, 101501C (2016).
18) L. Li, X. Yuan, N. Sun, H. Zhang, Y. Lai, X. Zhang, and M. Cao, Optik **125**, 1888 (2014).
19) Y. Zhang, X. Tian, L. Xue, Q. Zhang, L. Yang, and B. Zhu, IEEE Photonics Technol. Lett. **25**, 560 (2013).
20) P. Wang, G. Brambilla, M. Ding, Y. Semenova, Q. Wu, and G. Farrell, Opt. Lett. **36**, 2233 (2011).
21) J. Huang, X. Lan, H. Wang, L. Yuan, T. Wei, Z. Gao, and H. Xiao, Opt. Lett. **37**, 4308 (2012).
22) G. Numata, N. Hayashi, M. Tabaru, Y. Mizuno, and K. Nakamura, IEEE Photonics J. **6**, 6802306 (2014).
23) G. Numata, N. Hayashi, M. Tabaru, Y. Mizuno, and K. Nakamura, Appl. Phys. Express **8**, 072502 (2015).
24) T. Kawa, G. Numata, H. Lee, N. Hayashi, Y. Mizuno, and K. Nakamura, IEICE Electron. Express **14**, 20161239 (2017).
25) M. G. Kuzyk, *Polymer Fiber Optics: Materials, Physics, and Applications* (CRC Press, Boca Raton, FL, 2006).
26) Y. Koike and M. Asai, NPG Asia Mater. **1**, 22 (2009).
27) K. Koike, H. Teng, Y. Koike, and Y. Okamoto, Polym. Adv. Technol. **25**, 204 (2014).
28) N. Zhong, Q. Liao, X. Zhu, M. Zhao, Y. Huang, and R. Chen, Sci. Rep. **5**, 11508 (2015).
29) A. Pospori, C. A. F. Marques, M. G. Zubel, D. Saez-Rodriguez, K. Nielsen, O. Bang, and D. J. Webb, Proc. SPIE **9886**, 98860V (2016).
30) Y. Mizuno and K. Nakamura, Appl. Phys. Lett. **97**, 021103 (2010).